白質が多い.

なお，この単語は元来 chaperon という綴りであったが，原義が女性の持ち物あるいは女性自身をさすことが多かったことから，次第に cheperone という女性形単語として使われるようになった(OED). そして現代医学辞書はほとんどすべて chaperone という見出し語になっている. 筆者もこの流れに沿って, chaperone という綴りを使うことにしている.

I. ライソゾーム病の分子病態

ライソゾームはわれわれの細胞内に存在し，多くの高分子代謝産物を消化する小胞である. その内部は他のコンパートメントとは異なり，酸性である. ここで数十の加水分解酵素が一定の順序で化合物を分解してゆく. それぞれの酵素は特異的な遺伝子の情報により，細胞内で合成される. ある一つの遺伝子に構造異常(変異)が起こると，その間違った情報により産生された酵素の構造も変化し，変異蛋白質として活性を失い，細胞の機能障害を起こす. そして個体としては生後ある一定の時期に発病する. このグループの病気をまとめて(遺伝性)ライソゾーム病という. 主に小児期の進行性中枢神経疾患としての病像を示す. その臨床や病理，診断法などについては，筆者のいくつかの前著や標準的な教科書を参照していただきたい[1)~4)].

ライソゾーム酵素は赤血球以外，すべての体細胞に活性が存在するので，脳の病気であっても，その病態解析には，ほかの組織・臓器の細胞を使うことができる. われわれは，モデル細胞として，皮膚由来の線維芽細胞や末梢血由来のリンパ芽球などを用いた分析を，いくつかのライソゾーム酵素を発現する遺伝子について行ってきた. そして変異酵素の蛋白質を詳細に分析することにより，いわゆる「酵素欠損」の分子病態が一様でないことを知った.

大きく分けると次の3つに集約できる[5)]. 第1に蛋白質分子が合成されない場合. 第2に合成された蛋白質分子に酵素としての活性がない場合. 第3に活性のある酵素蛋白質は合成されるが，細胞内で不安定であり，すぐ分解されてしまう場合.

第1，第2の病態では正常な酵素蛋白質あるいは遺伝子を補給しない限り，細胞の機能を正常化することは不可能である. しかしこのアプローチは現在のところ，とくに脳組織については成功例がない. 第3の場合は，せっかく合成された酵素蛋白質を細胞がうまく利用できないという状況であり，何とかしてこの蛋白質に適切な細胞内環境を作ることができれば，潜在的に存在する酵素活性を復元し，細胞の機能を修復することができるはずである.

そこでわれわれはこの方向へのアプローチが可能であるかどうか，この10年余り，まず α-ガラクトシダーゼ欠損症（ファブリー病）に，ついで β-ガラクトシダーゼ欠損症（G_{M1}-ガングリオシドーシス，モルキオB病）の欠損酵素に対する実験的アプローチを行ってきた.

II. ケミカルシャペロン療法の原理

分析や実験の詳細は省略するが，ライソゾーム酵素が認識する基質の末端に存在する糖質，たとえば(α-または β-)ガラクトシダーゼであればガラクトース，(α-または β-) グルコシダーゼであればグルコースの類似化合物が，試験管内では競合的阻害剤として働く可能性がある. ライソゾーム酵素について調べたところ，一部の患者の変異蛋白質は，細胞内で合成された場所（中性）では不安定であった.

ところがこれらの細胞に試験管内阻害剤である基質類似化合物を投与すると，変異蛋白質と結合し，その立体的な折りたたみ(フォールディング）を助けることにより安定化し，そのまま

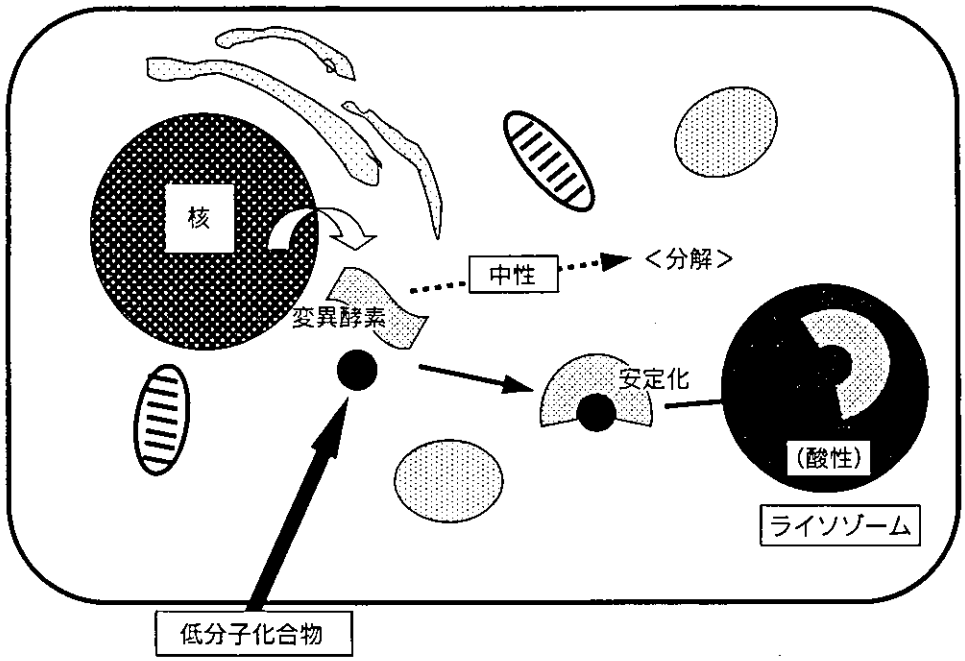

図1 ケミカルシャペロン療法の原理（遺伝性ライソゾーム病）
細胞の外から投与された低分子競合的阻害剤は細胞内に入り，標的となる変異蛋白質と結合し安定な立体構造を確立したあと，複合体がライソゾームに運ばれ，酸性の条件下で解離した変異蛋白質は酵素としての活性を発現する．

無事にライソゾームに送り届けることができた．ライソゾームの酸性条件では酵素蛋白質と投与した化合物は解離し，変異酵素は安定な状態で活性を発現する．

このような化合物は，上記の分子シャペロンと本質的に同じ働きをもつので，ケミカルシャペロン（chemical chaperone）とよぶことができる．その具体的な細胞内での分子反応のプロセスを図1の模式図に示す．

この細胞処理では，変異酵素活性を正常のレベルまで上昇させることができるとは限らない．しかし酵素の基質処理能力がある程度以上になれば，理論上は病気の発症を著しく遅らせることができることが予測できる．β-ガラクトシダーゼ欠損症についてのデータを整理すると図2のようになる[5]．正常活性の10%程度の活性が得られれば，発症年齢は無限大になる．つまり個体の生存中は発症しないということである．したがって，不十分な活性発現の細胞に対して，いくらかでも活性をあげることができれば，この目的が達成される可能性がある．

III. ファブリー病における欠損酵素復元の試み

変異α-ガラクトシダーゼの詳細な分析により，ファブリー病症例の一部に，細胞内の変異蛋白質が本来の酵素活性をもっているにもかかわらず，合成された中性の環境では分子として不安定であり，速やかに分解されてしまい，ライソゾームに運ばれないこと，そしてライソゾームの酸性環境では分子が安定で，活性を発現する可能性のあることがわかった．

そこで培養細胞に酵素が認識する基質の末端にあるガラクトースを投与してみたら，実際に活性が著しく増加した[6]．しかしこの実験に用いたガラクトースは高濃度であり，人体における血液の浸透圧よりも高い濃度にする必要があった．幸い，ほかの類似体のスクリーニング

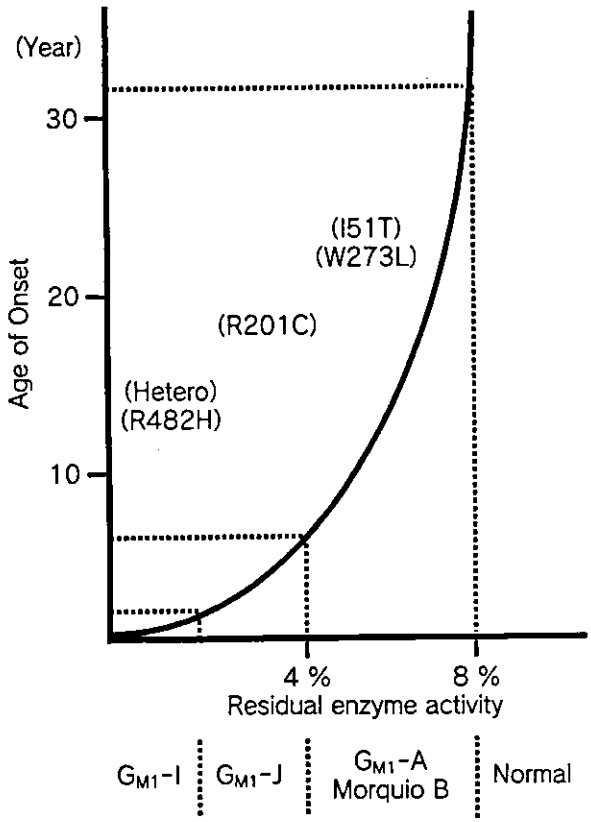

図2 β-ガラクトシダーゼ欠損症における発症年齢と線維芽細胞内残存活性との相関（鈴木義之，2002[5]）

G_{M1}-I：乳児型 G_{M1}-ガングリオシドーシス
G_{M1}-J：若年型 G_{M1}-ガングリオシドーシス
G_{M1}-A：成人型 G_{M1}-ガングリオシドーシス
Morquio B：モルキオ B 病
normal：正常人

これは線維芽細胞の酵素活性を非生理的な合成基質で評価した結果をまとめた曲線であり，ひとつの理論モデルとして理解していただきたい．脳の細胞におけるガングリオシド分解がまったく同じ曲線を描くかどうかはわからない．もちろん患者グループ内での個体差も考慮しなければならない．

の結果，市販の化合物，1-デオキシガラクトノジリマイシンがより低濃度でこの酵素の変異体に働くことがわかり，培養リンパ芽球，変異遺伝子導入で実際に活性が上昇することを確認した[7]．

この成果はそれ自体重要であるが，われわれにとっての最終目標は遺伝病の脳病変に対する治療的アプローチであり，全身血管病であるファブリー病ではこの点についての分析ができないという問題があった．そこで次に β-ガラクトシダーゼ欠損症，つまり古典的な遺伝性代謝性脳変性疾患である G_{M1}-ガングリオシドーシスを対象とした研究を始めた．

IV. 新しい β-ガラクトシダーゼ阻害剤 NOEV

この酵素の欠損症は，同一の遺伝子の異なった変異により，重症脳障害を起こす全身疾患（G_{M1}-ガングリオシドーシス）と骨系統疾患（モルキオ B 病）として発現する[8][9]．脳をはじめとして全身臓器にガングリオシド G_{M1}，そのアシアロ体 G_{A1} のほかにオリゴ糖やムコ多糖（ケラタン硫酸）などが蓄積する．

われわれはまず，市販のガラクトース誘導体・類似体について，この酵素の阻害活性を調べてみた．α-ガラクトシダーゼにかなり有効であった 1-デオキシガラクトノジリマイシンに対して，β-ガラクトシダーゼに対する阻害活性はその数十分の一であった．ほかの市販類似化合物でもこれ以上の活性を検出できなかった[10]．

そこで新しい化合物の検索を行うことにした．幸い生化学工業株式会社中央研究所のご協力により，新規合成化合物のスクリーニングを始めることができた．いくつかの化合物のなかで，N-オクチル-4-エピ-β-バリエナミン（N-octyl-4-epi-β-valianamine：NOEV）という化合物が試験管内で β-ガラクトシダーゼ活性の強力な阻害剤として働くことがわかった[11]．この物性解析の結果を図3に示す．この化合物はガラクトースの構造に似ているが，ガラクトースの C1 と C5 の間は O（酸素）結合でなく C（炭素）結合であり，かつ，C1 には O（酸素）でなく N（窒素）が結合しているという違いがある．現在までに，側鎖の炭素数 8 の化合物

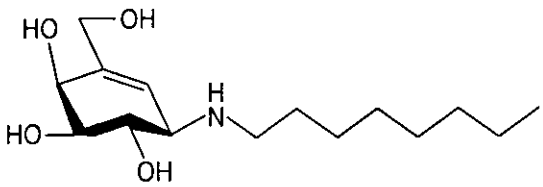

N-オクチル-4-エピ-β-バリエナミン
(NOEV)

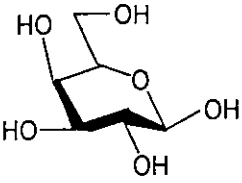

ガラクトース

1. 分子量 287.40
2. 室温で安定
3. 水 (3 mM),メタノール,DMSO に溶解
4. 試験管内：酵素活性を阻害 (競合的-高濃度：IC_{50}=0.2 μM)
5. 細胞内：酵素活性を復元 (低濃度)

図3 NOEV の構造と物性

コア構造はガラクトースに似ているが，ガラクトースのC1側鎖基部とC1～5結合部はガラクトースと異なる．

(NOEV) がわれわれの目的にもっとも有効であることを確認した．

この化合物には炭化水素側鎖がついているため，水に対する親和性は高くない．しかしこのフリー体のままでも 3～5 mM 濃度であれば容易に水に溶解する．室温で安定であり，試験管内での 50%酵素阻害濃度は 0.2 μM である．この化合物をヒト β-ガラクトシダーゼ欠損症患者由来の線維芽細胞培養液に添加すると，特定の変異遺伝子に対して活性化効果のあることがわかった．

V. β-ガラクトシダーゼ欠損症に対するケミカルシャペロン療法の試み

上記の予備的な結果をもとに，ヒト線維芽細胞，マウス線維芽細胞，われわれが開発したモデルマウス個体に対してこの薬剤投与実験を開始した．その成果は最近のわれわれの報告[11]にまとめた．

1．ヒト線維芽細胞

ヒト患者由来線維芽細胞の培養液に 0.2～2 mM の濃度に NOEV を添加し，4 日間培養したところ，酵素活性が著しく上昇する細胞株があった．とくに若年型あるいは成人型症例にみられる R 201 C，R 201 H 変異ではその反応が大きかった．全体として若年型症例にもっとも有効であり，乳児型，成人型症例にも 3 倍以上の活性上昇を示す症例があった．すべての症例をあわせて 30%の細胞が陽性反応を示した．モルキオ B 病にははっきりした反応がみられなかった．

2．マウス線維芽細胞

すでに確立し，報告した β-ガラクトシダーゼ欠損ノックアウトマウス[12)13)]の線維芽細胞を培養し，それにヒト β-ガラクトシダーゼ欠損患者の病型特異的な変異をもつ cDNA を導入して，この変異を発現する細胞株を確立した[10]．これらの細胞の培養液に NOEV を投与したところ，ヒト細胞とは多少の違いがあるが，ファブリー病で確認した 1-デオキシガラクトノジリマイシンの 1,000～2,000 倍の活性化効果を認めた．そしてやはり R 201 C 変異がもっとも有効であった[11]．

この培養系にガングリオシドを負荷したところ，正常遺伝子を発現する細胞には基質の蓄積がみられなかったのに対し，R 201 C 発現細胞ではガングリオシド G_{M1} とそのアシアロ体 G_{A1}

表 G_{M1}-ガングリオシドーシスモデルマウスへのNOEV投与効果

NOEV濃度	大脳	小脳	心	肺	肝	脾	腎	精巣 卵巣	筋肉
0 mM	5.3	8.7	12.0	8.1	23.6	8.6	35.4	26.6	3.6
0.1 mM	9.6	13.5	79.3	50.6	165.8	48.9	119.8	194.3	14.0
1 mM	24.4	28.6	225.8	114.9	165.2	142.4	183.4	195.1	61.6

マウス：R 201 C変異酵素を発現するノックアウト・トランスジェニックマウス
NOEV：水溶液としてアドリブに1週間投与
数字はβ-ガラクトシダーゼ活性：nモル/mg蛋白質/30分
脳を含むすべての組織でNOEV濃度依存的に著しい酵素活性上昇を認めた.

の著しい蓄積を示した. そして培養液にNOEVを添加したところ，これらの基質が著しく減少した[11].

これらの結果を踏まえ，以後の実験はR 201 C変異を対象とした実験を行った.

3．モデルマウスの作成と個体へのNOEV投与

動物個体実験のために，まず上記のノックアウトマウスにR 201 Cその他のヒトβ-ガラクトシダーゼ欠損症の病型特異的な変異遺伝子をトランスジーンとして導入したモデルマウスを作成した.

このなかで，正常なβ-ガラクトシダーゼを発現する遺伝子GP 8を導入したマウスは病気を発現せず，まったく正常の個体として生存した. つまり，この遺伝子過剰発現系の動物個体については遺伝子治療ができたということになる. 全身病に対する遺伝子治療は困難であるが，このアプローチであれば操作は容易である. もちろん，この結果をすぐにヒト個体に適用するわけにはいかないが，理論的には操作が可能であるということになる. ただしヒトのように生存期間が長い個体では，トランスジーンによる長期の酵素活性過剰発現の影響を考慮しなければならない.

次にR 201 CマウスにNOEVの1 mM水溶液を1週間経口投与した. 脳を含むすべての組織の酵素活性が著しく上昇し（表），病理学的，免疫組織化学的にも，脳組織のガングリオシド蓄積が消失した. これは発症前のマウス実験であり，臨床効果を観察することはできなかったが，今後は発症前から長期の薬剤投与を行い，発症予防効果があるかどうか検討する必要がある.

VI. NOEVについてわかったこと，検討すべきこと

以上の細胞，動物個体の実験から，次のようなことがわかった.

① 低分子化合物NOEVが腸管内で吸収され，血液に入り，血液脳関門を通って脳組織に入ること：これは現在試みているNOEVの血液内，組織内濃度の定量的測定によっても確かめられた. つまり，これまでに試みられたことのない，脳の遺伝病に経口薬を投与するという新しい治療的アプローチが理論的に可能となったということである.

② 培養細胞実験で確認されたように，NOEVが脳細胞のなかで変異蛋白質を安定化，活性化し，実際に異常に蓄積した基質（脂質）を分解すること：ガングリオシドG_{M1}もそのアシアロ体もともに分解された. 今回は1 mMという一定の濃度での実験データであるが，今後は投与量や投与方法による効果の違いが出るか

どうかを検討する.

③ NOEV の臨床効果：形態的，化学的分析により確かめた治療効果が，実際に臨床症状を修飾し，発症を予防し，症状を軽快させることの確認が必要である．現在検討中である.

④ NOEV が安定な化合物であること：これまでの実験では長期間，室温でまったく変化しないことがわかった．これは薬剤としての必須の条件であり，さらに安定性についての吟味を続ける.

⑤ 毒性の検討：薬剤として開発するためには，効果だけでなく長期投与に伴う毒性の検討が必須である．これまでのところ，5週間までは，体重，飲水量，血液生化学などにみるべき変化はなかった．さらに長期の投与による影響を確認する.

⑥ より有効な化合物の検索：NOEV がわれわれの目的にもっとも優れた化合物であるという保証はない．現在，いくつかの化合物をテスト中である．なかには同程度の活性をもち，かつ薬剤としての物性が優れている化合物もある.

⑦ NOEV の変異遺伝子特異的な効果：この化合物がすべての変異蛋白質に有効であるわけではない．変異遺伝子が分子として活性をもつ変異蛋白質を発現する，という条件が必須である．つまり同じ名前の病気のすべての患者に一様に適用できる手法ではない．しかし，現在まったく治療法のない病気の一部でもこの方法で症状の軽減，予防が可能になれば，きわめて大きな学問的，社会的な意味をもつ.

VII. 他のライソゾーム病・他の遺伝病への応用

すでに述べたように，この研究はファブリー病から始まった．現在の主要な研究対象は脳病変を発現する β-ガラクトシダーゼ欠損症候群，すなわち G_{M1}-ガングリオシドーシスである．モルキオ B 病については効果が確認できていない．しかし原理的にこのアプローチはすべてのライソゾーム病に適用できるはずである．実際，β-グルコシダーゼ欠損症候群（ゴーシェ病）でも，グルコース類似の化合物が，少なくとも培養細胞で有効であることが確認できている[14]．また α-ガラクトシダーゼに有効な NOEV 類縁体も検索中である.

このように，現在のところ，ガラクトースとグルコースの α および β 結合を認識する酵素についての分析が進行中であるが，今後はほかのライソゾーム酵素欠損症について，順次対象を広げる予定である.

たまたまわれわれはライソゾーム病という細胞内分子病態がかなり明らかにされた疾患群を対象としてきたが，ほかのカテゴリーの遺伝病でも，もしその分子病態，つまり変異遺伝子の発現，変異蛋白質の分子修飾，活性発現部位への細胞内移動，活性発現機構などが明らかにされれば，同じ原理の治療的アプローチが可能になるはずである.

その意味で，この分子治療法，ケミカルシャペロン療法が，今後多くの病気について検討され，実用化されることを期待している.

本稿の β-ガラクトシダーゼ欠損症の研究は国際医療福祉大学をはじめ，以下の多くの施設の研究者との共同研究により進行中である．黒澤美枝子(国際医療福祉大学基礎医学研究センター)，岩崎博之，渡辺浩史（国際医療福祉大学臨床医学研究センター)，松田潤一郎(国立感染症研究所獣医科学部)，難波栄二(鳥取大学生命機能研究支援センター)，大野耕策（鳥取大学医学部)，飯田真己(生化学工業中央研究所)，小川誠一郎（慶應義塾大学理工学部)．以上の代表者とともに，各施設の多くの共同研究者のご協力をいただいた．また α-ガラクトシダーゼ欠損症の研究には石井達（東京都臨床医学総合研究所，現・帯広畜産大学）と樊建強（東京都臨床医学総合研究所，現・マウントサイナイ医科大学）両氏の貢献が大きい．ここに

記して感謝の意を表する．この研究は文部科学省科学研究費（13680918，14207106）ならびに厚生労働省科学研究費（10030501，14221201）の補助金を受けた．

文 献

1) 鈴木義之：遺伝性ライソゾーム病の病態と分子病理．日本先天代謝異常学会雑誌 **11**：11-18，1995
2) 鈴木義之：リソソーム病総論．井村裕夫ほか（編）；最新内科学大系 11．ミトコンドリア病・リソソーム病，中山書店，pp 173-186，1996
3) 鈴木義之：遺伝性ライソゾーム病．内科 **87**：737-742，2001
4) Scriver CR et al (eds)：The Metabolic and Molecular Bases of Inherited Disease，8 th ed，2001，Online Version http：//genetics.accessmedicine.com/，2002-2004，McGraw-Hill，New York
5) 鈴木義之：β-ガラクトシドーシス：新しい分子治療法の開発．神経進歩 **46**：851-858，2002
6) Okumiya T et al：Galactose stabilizes various missense mutants of α-galactosidase in Fabry disease. Biochem Biophys Res Commun **214**：1219-1224，1995
7) Fan JQ et al：Accelerating transport and maturation of lysosomal α-galactosidase A in Fabry lymphoblasts by an enzyme inhibitor. Nature Med **5**：112-115，1999
8) Yoshida K et al：Human β-galactosidase gene mutations in G_{M1}-gangliosidosis；A common mutation among Japanese adult/chronic cases. Am J Hum Genet **49**：435-442，1991
9) Oshima A et al：Human β-galactosidase gene mutations in Morquio B disease. Am J Hum Genet **49**：1091-1093，1991
10) Tominaga L et al：Galactonojirimycin derivatives restore mutant human β-galactosidase activities expressed in fibroblasts from enzyme-deficient knockout mouse. Brain Dev **23**：284-287，2001
11) Matsuda J et al：Chenical chaperone therapy for brain pathology in G_{M1}-gangliosidosis. Proc Natl Acad Sci USA **100**：15912-15917，2003
12) Matsuda J et al：Neurological manifestations of knockout mice with β-galactosidase deficiency. Brain Dev **19**：19-20，1997
13) Matsuda J et al：β-Galactosidase-deficient mouse as an animal model for G_{M1}-gangliosidosis. Glycoconjugate J **14**：729-736，1997
14) Lin H et al：N-Octyl-β-valienamine upregulates activity of F 213 I mutant β-glucosidase in cultured cells；A potential chemical chaperone therapy for Gaucher disease. Biochim Biophys Acta **689**：219-228，2004

Available online at www.sciencedirect.com

SCIENCE DIRECT

Biochimica et Biophysica Acta 1689 (2004) 219–228

BIOCHIMICA ET BIOPHYSICA ACTA
BBA

www.bba-direct.com

N-Octyl-β-valienamine up-regulates activity of F213I mutant β-glucosidase in cultured cells: a potential chemical chaperone therapy for Gaucher disease

Hou Lin[a,1], Yuko Sugimoto[b], Yuki Ohsaki[b], Haruaki Ninomiya[b], Akira Oka[a], Miyako Taniguchi[b], Hiroyuki Ida[c], Yoshikatsu Eto[c], Seiichiro Ogawa[d], Yuji Matsuzaki[e], Miwa Sawa[e], Takehiko Inoue[a], Katsumi Higaki[f], Eiji Nanba[f], Kousaku Ohno[a,*], Yoshiyuki Suzuki[g]

[a] *Department of Neurobiology, Division of Child Neurology, Tottori University Faculty of Medicine, 86 Nishi-machi, Yonago 683-8504, Japan*
[b] *Department of Neurobiology, Tottori University Faculty of Medicine, Yonago 683-8503, Japan*
[c] *Departments of Pediatrics and Gene Therapy, Institute of DNA Medicine, Jikei University, Tokyo 105-8461, Japan*
[d] *Department of Applied Chemistry, Faculty of Science and Technology, Keio University, Yokohama 223-8522, Japan*
[e] *Central Research Laboratories, Seikagaku Corporation, Tokyo 207-0021, Japan*
[f] *Gene Research Center, Tottori University, Yonago, 683-8503, Japan*
[g] *Clinical Research Center, International University of Health and Welfare, Otawara 324-8501, Japan*

Received 3 October 2003; received in revised form 22 March 2004; accepted 25 March 2004
Available online 22 April 2004

Abstract

Gaucher disease (GD) is the most common form of sphingolipidosis and is caused by a defect of β-glucosidase (β-Glu). A carbohydrate mimic *N*-octyl-β-valienamine (NOV) is an inhibitor of β-Glu. When applied to cultured GD fibroblasts with F213I β-Glu mutation, NOV increased the protein level of the mutant enzyme and up-regulated cellular enzyme activity. The maximum effect of NOV was observed in F213I homozygous cells in which NOV treatment at 30 μM for 4 days caused a ~ 6-fold increase in the enzyme activity, up to ~ 80% of the activity in control cells. NOV was not effective in cells with other β-Glu mutations, N370S, L444P, 84CG and RecNciI. Immunofluorescence and cell fractionation showed localization of the F213I mutant enzyme in the lysosomes of NOV-treated cells. Consistent with this, NOV restored clearance of ^{14}C-labeled glucosylceramide in F213I homozygous cells. F213I mutant β-Glu rapidly lost its activity at neutral pH in vitro and this pH-dependent loss of activity was attenuated by NOV. These results suggest that NOV works as a chemical chaperone to accelerate transport and maturation of F213I mutant β-Glu and may suggest a therapeutic value of this compound for GD.
© 2004 Elsevier B.V. All rights reserved.

Keywords: Gaucher disease; β-glucosidase; Valienamine; Glucosylceramide; Chaperone

1. Introduction

Gaucher disease (GD) is an inherited lipid storage disorder, characterized by lysosomal accumulation of glucocerebroside (glucosylceramide; GlcCer) in monocyte-macrophage cells [1]. It is caused by a defect of acid β-glucosidase (β-Glu; glucocerebrosidase EC 3.2.1.45). Patients with GD exhibit hepatosplenomegaly, anemia, bone lesions and respiratory failure, with or without progressive neurological symptoms. Patients without neurological symptoms are classified as type 1, whereas those with neurological symptoms are classified into type 2 (acute infantile form) and type 3 (juvenile form).

Abbreviations: α-Gal A, α-galactosidase A; α-Glu, α-glucosidase; β-Gal, β-galactosidase; β-Glu, β-glucosidase; β-Hex, β-hexosaminidase; NOEV, *N*-octyl-β-epi-valienamine; NOV, *N*-octyl-β-valienamine; DGJ, 1-deoxy-galactonojirimycin; ER, endoplasmic reticulum; GD, Gaucher disease; GlcCer, glucosylceramide; HPTLC, high performance thin layer chromatography; NN-DGJ, *N*-(*n*-nonyl)-deoxy-nojirimaycin

* Corresponding author. Tel.: +81-859-34-8037; fax: +81-859-34-8135.
E-mail address: ohno@grape.med.tottori-u.ac.jp (K. Ohno).
[1] Present address: Department of Biochemistry, Medical College, Qingdao University, Qingdao, Shandong 266021, PR China.

0925-4439/$ - see front matter © 2004 Elsevier B.V. All rights reserved.
doi:10.1016/j.bbadis.2004.03.007

Current therapeutic strategies for GD include enzyme replacement and substrate depletion. Enzyme replacement has been achieved by intravenous administration of macrophage-targeted recombinant β-Glu [2] and it has been proven to be quite effective for visceral, hematologic and skeletal abnormalities [3,4]. Unfortunately, the efficacy to neurological manifestations of this therapy is, if any, limited [5–7]. A high cost as well as necessity to continue the infusion every 2 weeks is not negligible, when indication of enzyme replacement is considered in practice [4]. Substrate depletion has been achieved by oral administration of *N*-butyl-deoxynojirimycin, which inhibits glucosyltransferase and decreases substrate biosynthesis. This therapy has been reported to be beneficial for non-neuropathic GD [8,9].

We have proposed a novel therapeutic strategy for glycolipid storage disorders to accelerate transport and maturation of mutant enzymes by using enzyme inhibitors as a chemical chaperone. This strategy was first applied to Fabry disease (α-galactosidase A [α-Gal A] deficiency) and we found that 1-deoxy-galactonojirimycin (DGJ), an inhibitor of α-Gal A, markedly enhanced activity of mutant enzymes in lymphoblasts from Fabry patients [10]. Although up-regulation of enzyme activity by an inhibitor appeared paradoxical, evidence was presented that DGJ prevented pH-dependent degradation of mutant α-Gal A at the site of its synthesis [i.e., the endoplasmic reticulum (ER)]. With the aid of DGJ, mutant α-Gal A escaped the ER quality control system and was transported to the lysosome where it is stabilized because of the acidic condition and restored cellular enzyme activity. This strategy was then tested in GM1-galactosidosis [β-galactosidase (β-Gal) deficiency] and we found that DGJ as well as another derivative *N*-(*n*-butyl)-deoxy-galactonojirimycin could up-regulate activity of mutant human β-Gal expressed in fibroblasts from β-Gal knockout mice [11]. In pursuit of the same therapeutic strategy, Sawkar et al. [12] reported that an inhibitor of β-Glu, *N*-(*n*-nonyl)-deoxynojirimaycin (NN-DNJ) up-regulated activity of N370S mutant β-Glu in GD fibroblasts. Although it is yet to be tested whether NN-DNJ can correct GlcCer accumulation in N370S GD cells, their findings suggested that this strategy might be extended to GD.

Valienamine is a synthetic carbohydrate mimic and we have prepared various *N*-alkyl and *N*,*N*-dialkyl-β-valienamines in continuation of a chemical modification program [13]. Among these substances, *N*-octyl-β-epivalienamine (NOEV) is an inhibitor of β-Gal and we have provided evidence that NOEV worked as a chemical chaperone to up-regulate mutant β-Gal activity both in cultured cells and in mice [14]. *N*-octyl-β-valienamine (NOV) is an isomer of NOEV and exerted the strongest inhibition of β-Glu activity in the mouse liver [15]. The purpose of the current studies was to test a possibility that NOV could up-regulate mutant β-Glu activity in cultured human cells. Preliminary findings of the current studies have been reported [16].

2. Materials and methods

2.1. Materials

Dulbecco's Modified Eagle's Medium (DMEM), fetal calf serum (FCS) and dialyzed serum were obtained from GibcoBRL. NOV was synthesized in our laboratory (Central Research Laboratories, Seikagaku). Stock solution of NOV was prepared in H_2O at 3 mM and stored at −20 °C. A mouse monoclonal antibody against human β-Glu (clone 8E4, Ref. [17]) was a kind gift from Dr. Barranger JA. Rabbit polyclonal anti-hexosaminidase A (HexA) has been described [18]. Rabbit polyclonal anti-calnexin was from Calbiochem. [1-^{14}C]Serine (1.85 GBq/mmol) was from American Radiolabeled Chemicals (St. Louis, MO).

2.2. Cell culture

Human skin fibroblasts were cultured in DMEM/10% FCS at 37 °C in 5% CO_2. We used two lines of control cells (H11, H34) and five lines of GD cells with β-Glu mutations of 754A(F213I)/754A(F213I), 754A(F213I)/1448C(L444P), 1126G(N370S)/84GG, 1448C(L444P)/RecNciI, and 1448C(L444P)/1448C(L444P) [19]. 84GG causes premature termination of the encoded protein and RecNciI causes amino acid substitutions L444P and A456P [1]. Culture medium was replaced every 2 days with fresh media supplemented with or without NOV at the concentrations indicated.

2.3. Enzyme assays

Lysosomal enzyme activities in cell lysates were determined as described [14,18,20,21]. Briefly, cells were scraped into ice-cold H_2O (10^6/ml) and lysed by sonication. Insoluble materials were removed by centrifugation at 12,000 × *g* for 10 min at 4 °C and protein concentrations were determined with a BCA microprotein assay kit (Piearce). Ten microliters of the lysates was incubated at 37 °C with 20 μl of the substrate solution in 0.1 M citrate buffer, pH 4.5. The substrates were 4-methylumbelliferone-conjugated β-D-galactopyranoside (for β-Gal, Ref. [14]), β-D-glucopyranoside (for β-Glu, Ref. [20]), α-D-glucoside (for α-Glu, Ref. [21]) and *N*-acetyl-β-D-glucosaminide (for β-Hex, Ref. [18]). The reaction was terminated by adding 1.0 ml of 0.2 M glycine sodium hydroxide buffer (pH 10.7). One unit of enzyme activity was defined as nanomoles of 4-methyl-umbelliferone released per hour.

2.4. Western blotting

Cell lysates (20 μg protein) were electrophoresed on a 10% SDS-PAGE and transferred to a PVDF membrane.

The blots were probed with antibodies against β-Glu (1:500) or HexA (1:1000) and developed with an ECL kit (Amersham Pharmacia). Densitometry was performed by using an NIH image software.

2.5. Immunofluorescence

We used staining procedures described previously [22]. Briefly, cells grown on cover glasses were fixed with 4% paraformaldehyde and permiabilized with 1% Triton X-100. Cells were incubated with anti-β-Glu (1:100), followed by Alexa488-conjugated anti-mouse IgG. Fluorescent images were collected by using a Bio-Rad MRC1024 confocal laser microscope. For localization of lysosomes, cells were exposed to Lysotracker Red (5 μg/ml; Molecular Probe) for 1 h prior to fixation.

2.6. Subcellular fractionation

Cell homogenates were fractionated by using Opti-prep (Axis-Shield plc., Dundee, UK) as described [23]. Briefly, cells were homogenized with a potter homogenizer in ice-cold buffer [HEPES 10 mM pH 7.0, 1 mM EDTA, 1 mM EGTA supplemented with a protease inhibitor cocktail (Boehringer)]. Homogenates were overlaid on Opti-prep and centrifuged at 100,000 × *g* for 16 h at 4 °C. Twelve fractions were recovered from the top and numbered accordingly.

2.7. Metabolic labeling of GlcCer

Cellular glycolipids were labeled with [^{14}C]serine as described [24]. Briefly, cells were cultured for 1 week in dialyzed serum supplemented with essential amino acids except for serine, and incubated with [^{14}C]serine (1 μCi/ml) for 3 days. The labeled cells were cultured in fresh DMEM/10% FCS for 5 days with or without NOV. We analyzed labeled lipids by high-performance thin layer chromatography (HPTLC) as described [25]. In brief, cells were harvested at the time indicated, and lipids were extracted with chloroform/methanol (2:1 v/v) and purified by an alkaline treatment. Neutral glycolipids were purified by C18 affinity chromatography. HPTLC was performed with chloroform/methanol/water (55:25:4) as a developing solvent. Labeled lipids were visualized by autoradiography (Fuji-BAS 2500: Fuji, Tokyo, Japan) and densitometry was performed using an NIH image software.

2.8. pH-dependent stability of β-Glu in vitro

Cell lysates were incubated in 0.1 M citrate-phosphate buffer at pH 5, 6 or 7 at 37 °C for the time indicated. Incubation was terminated by the addition of 3 volumes of 0.2 M citrate-phosphate buffer (pH 4.5), immediately followed by chilling on ice. The enzyme assay was done at pH 4.5 as described above.

3. Results

3.1. Inhibition of human β-Glu by NOV in vitro

Chemical structures of NOV and its isomer NOEV are shown in Fig. 1a. NOV inhibited β-Glu activity in mouse liver extracts with an IC_{50} value of 0.03 μM [15]. To test whether it also works on the human enzyme, we determined β-Glu activity in lysates from control human fibroblasts in the absence or presence of NOV. NOV caused dose-dependent inhibition of β-Glu activity with an IC_{50} value of 3 μM (Fig. 1b), indicating that it also works on human β-Glu. NOV contains a C8 fatty acid acyl moiety chain (Fig. 1a). A related compound with a C6

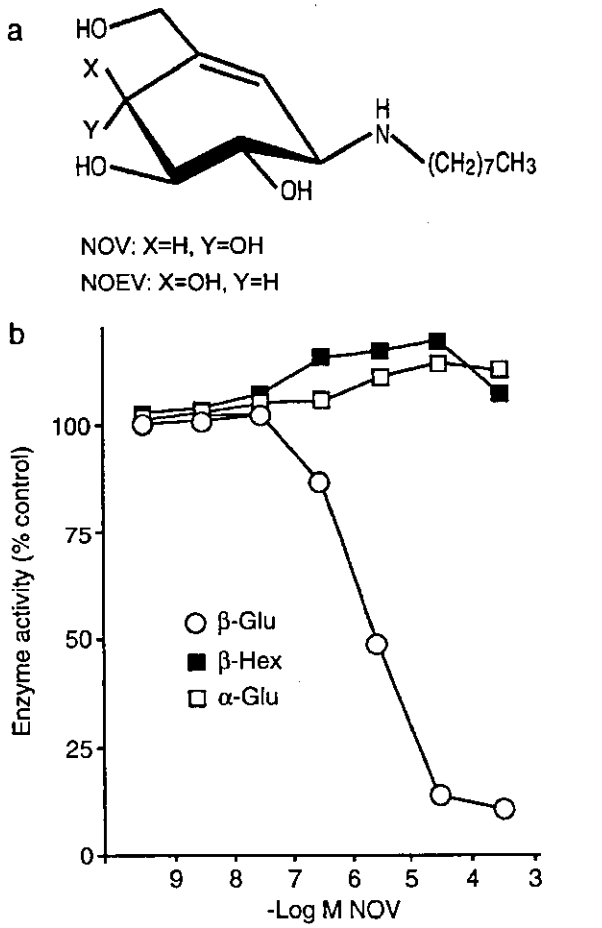

Fig. 1. Effects of NOV on lysosomal enzyme activities in lysates from control human fibroblasts. (a) Chemical structures of NOV and its isomer NOEV. (b) Dose dependence. Enzyme activity in H11 cell lysates was determined in the absence or presence of increasing concentrations of NOV. Each point represents means of triplicate determinations obtained in a single experiment. Values were expressed as relative to activity in the absence of NOV (100%). Values in the absence of NOV in this experiment were β-Glu 142, α-Glu 94 and β-Hex 5089 (units/mg protein). Similar results were obtained in two other experiments.

fatty acid acyl moiety chain inhibited human β-Glu with an IC_{50} value of 30 μM (data not shown), suggesting that the inhibitory activity can be regulated by the length of this chain. NOV caused no inhibition of other lysosomal enzymes α-Glu and β-Hex in the same cell lysates, suggesting a specificity of NOV as an inhibitor of β-Glu (Fig. 1b).

3.2. Up-regulation of F213I mutant β-Glu activity in GD cells treated with NOV

To explore an effect of NOV on mutant β-Glu activity, GD cells with five different genotypes were cultured for 4 days with increasing concentrations of NOV, and β-Glu activity in cell lysates was determined (Fig. 2a, right). NOV

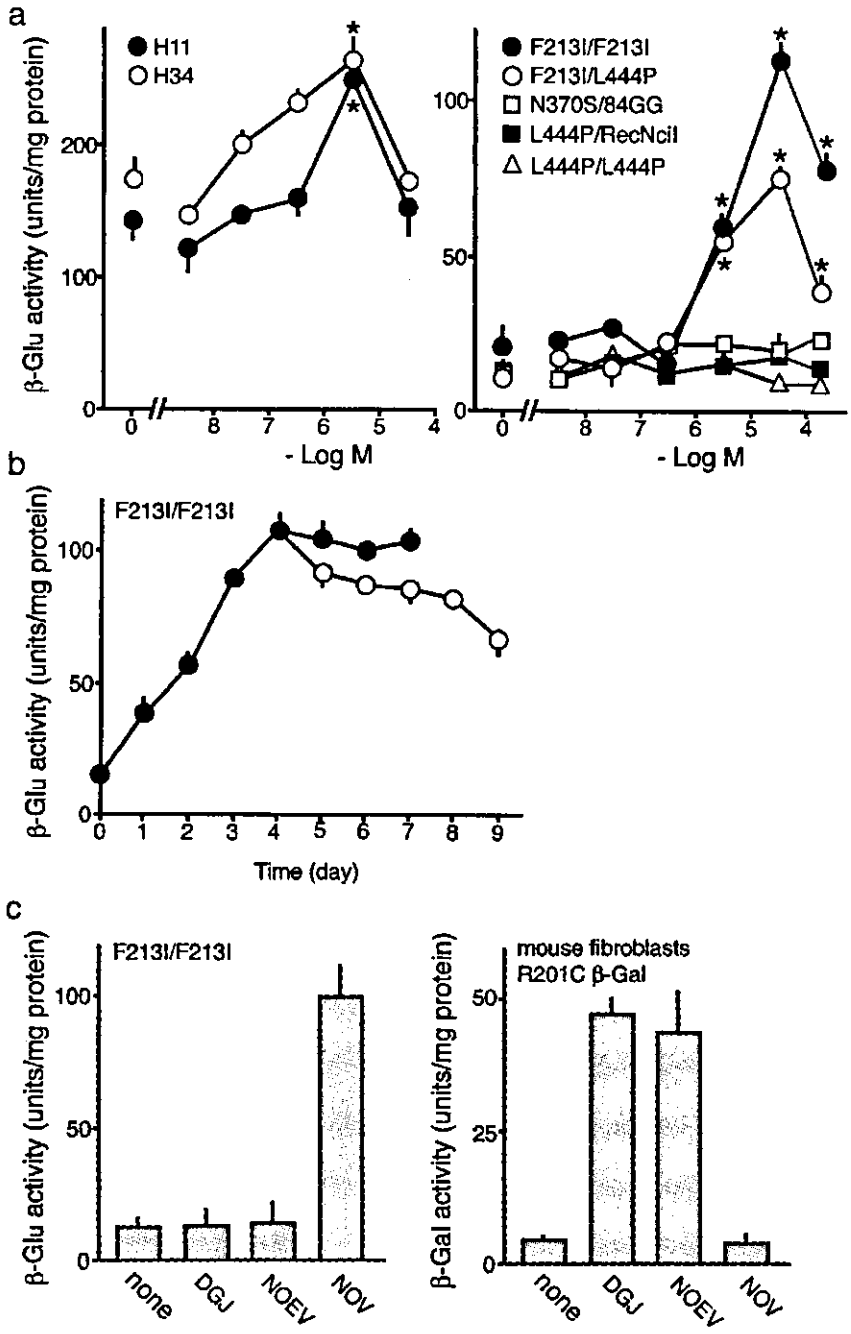

Fig. 2. Effects of NOV on cellular β-Glu activity. (a) Dose dependence. Two lines of control cells (left) and five lines of GD cells (right) were cultured for 4 days in the absence or presence of increasing concentrations of NOV and β-Glu activity in cell lysates was determined. (b) Time course. F213I/F213I cells were cultured in the presence of 30 μM NOV up to 7 days (●). A subset of cells was cultured with NOV for 4 days, washed and further cultured without the drug for 5 days (○). At the time indicated, cells were harvested and β-Glu activity in cell lysates was determined. (c) Specificity of the effects of NOV. F213I/F213I cells were cultured in the presence of indicated drugs (all at 20 μM) for 4 days and β-Glu activity in cell lysates was determined (left). In separate experiments, the same drugs were applied to mouse fibroblasts that express human R201C β-Gal and β-Gal activity in cell lysates was determined (right). Each point or bar represents mean ± S.E. of three determinations each done in triplicate. $^*P<0.05$, statistically different from the values in the absence of the drug (*t* test).

caused dose-dependent increases in β-Glu activity in two lines of GD cells, F213I/F213I and F213I/L444P. The maximum effect of NOV was observed in F213I homozygous cells in which treatment at 30 μM caused a ~ 6-fold increase in the enzyme activity, up to ~ 80% of the basal activity in control cells. NOV at the same concentration caused a ~ 3-fold increase in F213I/L444P cells. There appeared to be an optimal concentration of NOV, because it was less potent at a higher concentration (100 μM). NOV caused no substantial increase in the enzyme activity of GD cells with other mutations, indicating a specificity of this up-regulation for F213I mutant β-Glu. This effect of NOV, however, was also observed in wild-type β-Glu with a different dose dependence profile; NOV at 3 μM caused a ~ 1.5-fold increase in the two control cell lines but was not effective at 30 μM (Fig. 2a, left).

Time-course analysis using F213I/F213I cells showed that in the presence of NOV (30 μM), β-Glu activity increased in a time-dependent manner and reached a plateau on day 4. When cells were deprived of NOV on

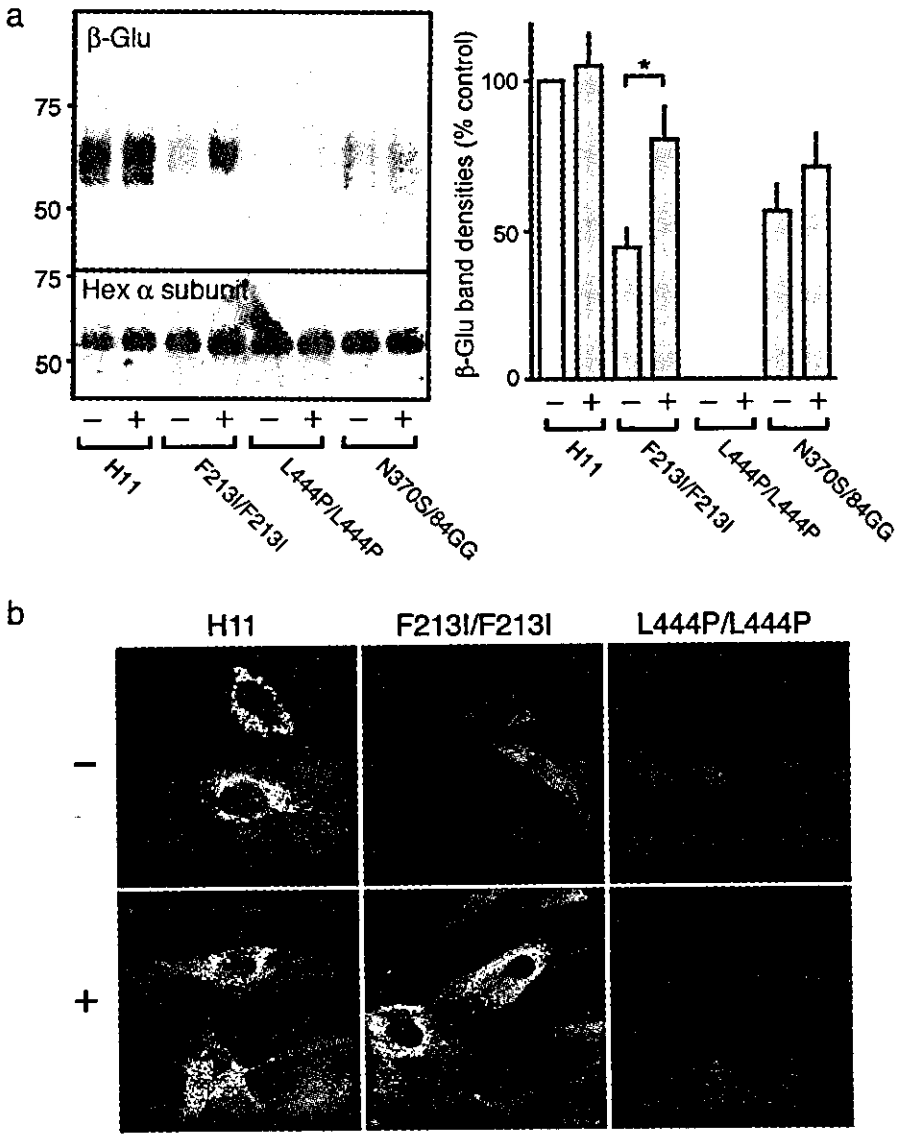

Fig. 3. Effects of NOV on the protein level and intracellular localization of mutant β-Glu. Cells were cultured with (+) or without (−) NOV at 30 μM for 4 days. (a) Western blotting. Cell lysates were analyzed by Western blotting with antibodies against β-Glu or Hex α subunit (left). Twenty micrograms of protein was loaded in each lane. Molecular weights are given on the left (kDa). Densities of β-Glu bands were quantified by densitometry (right). Each bar represents mean ± S.E. of 3 determinations. *$P<0.05$, statistically different from each other (t test). (b) Anti-β-Glu immunofluorescence. (c) Double labeling of F213I/F213I cells with anti-β-Glu and Lysotracker Red. In b and c, shown are the representative images obtained with a confocal microscope. All the images were obtained at the same laser intensity and window level. (d) Cell fractionation. Cells were cultured with (●) or without (○) NOV at 30 μM for 4 days. Cell homogenates were subjected to Opti-prep fractionation and each fraction was assessed for activity of β-Glu (upper) or β-Hex (lower). Fractions from F213I/F213I cells were also subjected to anti-calnexin Western blotting. Each point represents mean values of triplicate determinations obtained in a single experiment. Similar results were obtained in two other experiments.

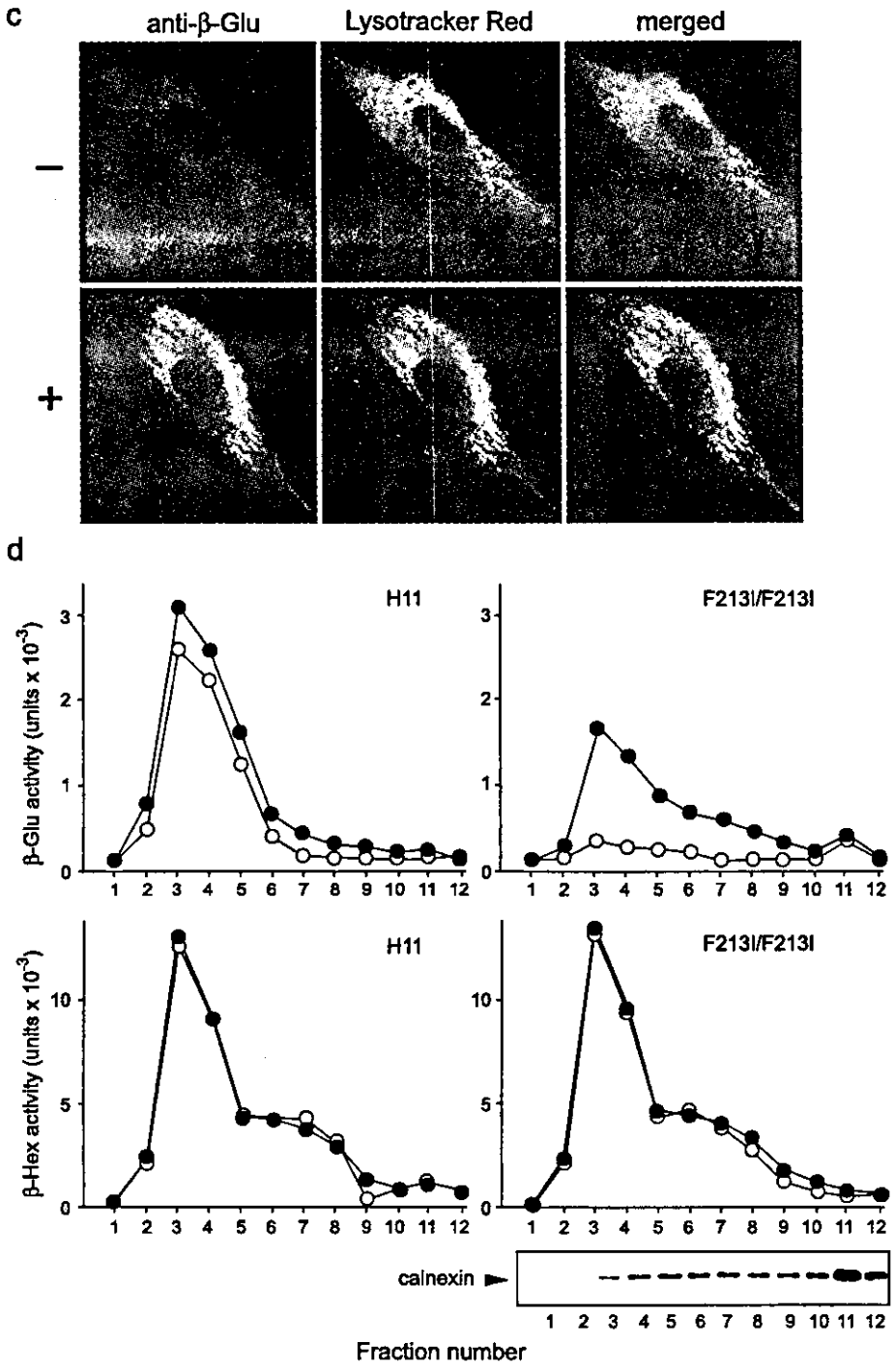

Fig. 3 (*continued*).

day 4, the activity gradually decreased thereafter but was still more than three times higher than the basal level on day 9 (Fig. 2b).

We have shown that both DGJ and NOEV could up-regulate the activity of R201C mutant β-Gal that was expressed in fibroblasts derived from β-Gal knockout mice [11,14]. To test specificity of NOV, first, we examined whether DGJ or NOEV could up-regulate F213I β-Glu activity, and found that neither of these substances caused any changes in the activity (Fig. 2c, left). Second, we examined whether NOV could up-regulate the activity of R201C mutant β-Gal, and found that unlike DGJ and NOEV, NOV had no effect on this mutant enzyme (Fig. 2c, right).

3.3. NOV increased the protein level of F213I mutant β-Glu and restored its localization in the lysosome

To examine the effect of NOV on the protein level, cell lysates were subjected to Western blotting with 8E4 monoclonal anti-β-Glu antibody and the protein levels were estimated by densitometry. This analysis showed that NOV treatment (30 μM for 4 days) of F213I/F213I cells caused a significant increase in the protein level of F213I mutant β-Glu. The same treatment did not increase the protein levels in N370S/84GG and control cells. As reported previously [26], the antibody did not recognize L444P mutant β-Glu. As a control, NOV treatment caused no changes in the protein levels of Hex α subunit (Fig. 3a).

Next, we examined intracellular localization of β-Glu by immunofluorescence and cell fractionation. Anti-β-Glu staining of control cells showed localization of β-Glu immunoreactivity in perinuclear punctate structures and this localization was not affected by NOV treatment. β-Glu immunoreactivity in F213I/F213I cells was lower than in control cells and there was no clear localization in perinuclear punctate structures. When these cells were treated with NOV, however, the immunoreactivity was clearly seen in these structures (Fig. 3b). Localization of F213I mutant β-Glu in the lysosome of NOV-treated cells was evidenced by co-localization of the immunoreactivity and a lysosome marker Lysotracker Red (Fig. 3c). β-Glu immunoreactivity was not detectable in L444P/L444P cells, indicating the specificity of this antibody staining (Fig. 3b).

When control cells were subjected to subcellular fractionation on Opti-prep, β-Glu activity was recovered in fractions #3–5. The same analysis of F213I/F213I cell fractions showed broad distribution of mutant β-Glu activity with peaks at #3 and #11. Both peaks were small but were consistently observed in three independent determinations. Anti-calnexin Western blotting showed that #11 contained a high amount of this ER marker protein [27]. NOV treatment of control cells caused marginal increases (~ 1.1-fold) in β-Glu activity recovered in #3–5. The same treatment of F213I/F213I cells caused ~ 4-fold increases in #3–5. As a control, we measured β-Hex activity in each fraction. Both in control and F213I/F213I cells, β-Hex activity was recovered in #3–4 and to a lesser degree, in #5–8. β-Hex activity in each fraction was not affected by NOV treatment in either cell line (Fig. 3d).

3.4. NOV restored clearance of ^{14}C-labeled GlcCer in F213I/F213I cells

NOV-induced increase of mutant β-Glu activity in the lysosome of F213I/F213I cells prompted us to examine whether NOV could correct abnormal catabolism of GlcCer in this cell line. By using conventional HPTLC analysis of cellular lipid extracts, accumulation of GlcCer was barely detectable in GD skin fibroblasts, most likely because of the low level of this lipid in these cells (data not shown). Therefore, we employed metabolic labeling of cellular glycolipids with [^{14}C]serine and assessed clearance of ^{14}C-labeled GlcCer. When control cells were chased for 5 days after the metabolic labeling, the content of ^{14}C-GlcCer decreased by ~ 50%. This clearance of ^{14}C-GlcCer was retarded in F213I/F213I cells in which there was only a ~ 10% decrease. Inclusion of NOV (30 μM) in the chase medium had no effect in control cells but accelerated the clearance in F213I/F213I cells. In the presence of NOV, the content of ^{14}C-GlcCer in F213I/F213I cells decreased by ~ 50% and reached a level that was comparable to that in control cells (Fig. 4b). The HPTLC analyses showed that besides ^{14}C-GlcCer, clearance of ^{14}C-LacCer was retarded in F213I/F213I cell and again it was accelerated by NOV (Fig. 4a). In addition, NOV caused decreases in the levels of ^{14}C-labeled lipids that corresponded to the positions of CTH, SM and

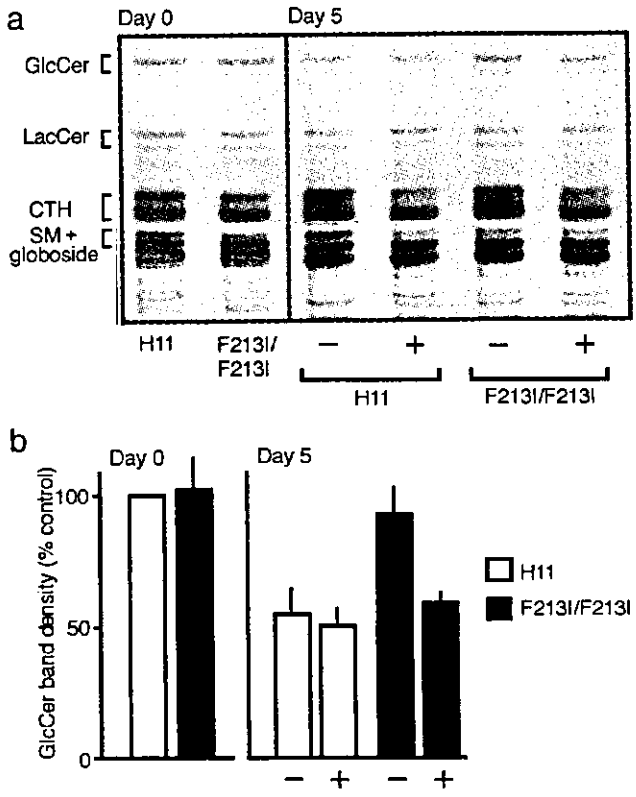

Fig. 4. Effects of NOV on cellular clearance of ^{14}C-labeled GlcCer. (a) HPTLC separation of ^{14}C-labeled cellular lipids. Cells were labeled with ^{14}C-serine for 3 days and then chased up to 5 days in the presence or absence of NOV (30 μM). At the beginning (day 0) and the end (day 5) of the chase period, cells were harvested and neutral glycolipid fraction was analyzed by HPTLC. Positions of standard lipids are given on the left (LacCer, lactosylceramide; CTH, ceramide trihexoside; SM, sphingomyelin). (b) Densitometry. Densities of ^{14}C-GlcCer bands on autoradiographs were quantified using an NIH image software. Values were expressed as relative to the band density of H11 cell extracts at the beginning of the chase period (day 0) as 100%. Each bar represents mean ± S.E. of three determinations.

globoside. The decreases, however, were observed both in control and F213I/F213I cells and the identities of these lipids were left unresolved.

3.5. NOV attenuated pH-dependent loss of F213I mutant β-Glu activity in vitro

Some mutations of lysosomal enzymes affect pH-dependent protein stability [1] and we reported that an α-Gal A inhibitor DGJ prevented in vitro degradation of mutant α-Gal A at neutral pH [10]. To examine whether a similar mechanism underlined NOV effects on F213I mutant β-Glu, we compared pH-dependent stability of wild-type and F213I mutant β-Glu and tested an effect of NOV. In these experiments, we used cell lysates prepared from untreated control cells and from F213I/F213I cells that had been treated with NOV at 30 μM for 4 days and further cultured without the drug for 1 day. When F213I/F213I cell lysates were incubated at pH 7, mutant β-Glu activity was rapidly lost and there remained less than 5% activity at 1 h. Mutant β-Glu activity also decreased in acidic conditions at pH 5 or 6, but ~ 60% activity retained at 1 h under these conditions. In contrast, there were only marginal decreases of wild-type β-Glu activity in control cell lysates and more than 80% activity retained after 1-h incubation at every pH (Fig. 5a). The decrease of F213I mutant β-Glu activity at neutral pH was attenuated by NOV in a dose-dependent manner (Fig. 5b).

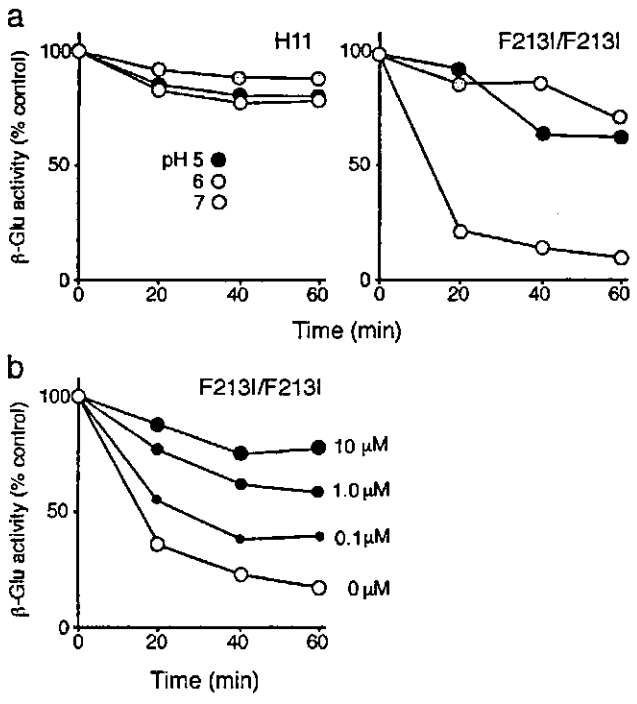

Fig. 5. Effects of NOV on pH-dependent loss of F213I mutant β-Glu activity in vitro. (a) Time course. Cell lysates were incubated at 37 °C in 0.1 M citrate-phosphate buffer at the indicated pH and the enzyme activity was determined at pH 4.5. (b) Effects of NOV. F213I/F213I cell lysates were incubated at pH 7 in the absence or presence of NOV at the concentrations indicated. Each point represents mean values of triplicate determinations obtained in a single experiment. Values were expressed as relative to the activity before the incubation (100%). Similar results were obtained in two other experiments.

4. Discussion

We found in the current study that, when applied to GD cells with F213I mutations, NOV up-regulated cellular β-Glu activity (Fig. 2) and accelerated cellular clearance of GlcCer (Fig. 4). NOV caused a modest but significant increase in the protein level of the mutant enzyme and increased its activity in the lysosome (Fig. 3). We also found pH-dependent loss of F213I mutant β-Glu activity in vitro and its prevention by NOV (Fig. 5). These findings are most likely explained by an activity of NOV as a chemical chaperone to accelerate transport and maturation of F213I mutant β-Glu. Although details are yet to be proven, we suppose that F213I mutant β-Glu is degraded in the ER because of its instability at neutral pH. With the aid of NOV, this mutant β-Glu is protected from degradation and is transported to the lysosome where it is stabilized because of the acidic condition and cellular enzyme activity is restored. Since effects of NOV on ER enzymes responsible for β-Glu degradation have not been examined, an alternative possibility remains to be excluded that the observed effects of NOV were secondary to inhibition of such enzyme(s). Although we have shown negative effects of NOV on some other lysosomal enzymes in vitro (Fig. 1b), potential effects of this compound on ER enzymes must be the subject of future studies.

Because NOV is an inhibitor of β-Glu (IC_{50} = 3 μM, Fig. 1b), it should inhibit β-Glu activity at the lysosome if it reaches to an appropriate concentration in this compartment. NOV was most effective in inducing F213I mutant β-Glu activity at 30 μM in the medium (Fig. 2a), which was 10 times higher than its IC_{50} value. NOV at this concentration, however, failed to inhibit ^{14}C-GlcCer clearance both in control and F213I/F213I cells (Fig. 4). One possible explanation for this apparent lack of inhibition is that at 30 μM in the medium, the concentration of NOV in the lysosome did not rise high enough to inhibit β-Glu activity (whereas the concentration in the ER did rise high enough to prevent mutant β-Glu degradation). If this is the case, the action of NOV as a β-Glu inhibitor may emerge at inappropriately high concentrations. Indeed, NOV was less effective at 100 μM in increasing F213I mutant β-Glu activity (Fig. 2a), although it is yet to be proven that it was due to this action of NOV. We noticed similar dose dependence for DGJ to increase mutant α-Gal A activity in Fabry lymphocytes [10]. Thus, it is apparent that there is an appropriate concentration range for an enzyme inhibitor to up-regulate cellular enzyme activities.

The effect of NOV on cellular enzyme activity was specifically observed in GD cells with F213I mutations

but not in cells with other point mutations N370S, L444P and RecNciI (L444P and A456P) (Fig. 2a). Although a precise molecular basis is left unknown, this selectivity might depend on the differences in the stability of individual enzymes, or alternatively, on the differences of NOV-binding capacities. In this context, the lack of NOV effects on N370S/84GG cells is in contrast to the reported effects of NN-DNJ that caused a twofold increase of β-Glu activity in N370S homozygous cells [12]. It should be clarified in future studies whether this difference in the effects of NOV and NN-DNJ is due simply to the cell lines employed, or to differential binding capacities of N370S mutant enzyme to these substances.

N370S is the most common mutation in GD patients and is associated only with type 1 non-neuronopathic GD [1]. F213I is one of the two prevalent mutations in Japanese GD patients, found in 15% of alleles [19]. Clinically, patients with F213I mutations have either non-neuronopathic or neuronopathic GD. NOV may be of particular therapeutic value in the latter group, since there is no established therapy against GD brain lesions. We have shown that NOEV, an isomer of NOV, could penetrate the blood–brain barrier in mice [14]. It must be determined in a future study whether NOV penetrates the blood–brain barrier and exerts its activity on mutant β-Glu in the brain.

Finally, besides F213I, other β-Glu mutant forms are a potential target of NOV or related compounds. In this context, it should be noted that in a report of a neuronopathic GD patient with G202R mutations, ultrastructural immunohistochemistry revealed the absence of the mutant protein in the lysosome, despite its abundant presence in the ER [28]. So far, nojirimycin derivatives have been an only known class of carbohydrate mimics with chemical chaperone activity for lysosomal enzymes [10–12]. Together with NOEV [14], NOV represents a novel class of carbohydrate mimics with a potential chemical chaperone activity. It is a subject of future studies to test whether NOV and related compounds work as a chemical chaperone for other β-Glu mutant forms, and further for other mutant lysosomal enzymes.

Acknowledgements

This work was supported in part by grant "Research on Psychiatric and Neurological disorders and Mental Health" from the ministry of Health, Labor and Welfare of Japan.

References

[1] E. Beutler, G.A. Grabowski, Gaucher disease, The Metabolic and Molecular Bases of Inherited Disease, McGraw-Hill, New York, 2001, pp. 2641–2670.

[2] N.W. Barton, R.O. Brady, J.M. Dambrosia, A.M. Di Bisceglie, S.H. Doppelt, S.C. Hill, H.J. Mankin, G.J. Murray, R.I. Parker, C.E. Argoff, et al., Replacement therapy for inherited enzyme deficiency—macrophage-targeted glucocerebrosidase for Gaucher's disease, N. Engl. J. Med. 324 (1991) 1464–1470.

[3] D.I. Rosenthal, S.H. Doppelt, H.J. Mankin, J.M. Dambrosia, R.J. Xavier, K.A. McKusick, B.R. Rosen, J. Baker, L.T. Niklason, S.C. Hill, et al., Enzyme replacement therapy for Gaucher disease: skeletal responses to macrophage-targeted glucocerebrosidase, Pediatrics 96 (1995) 629–637.

[4] G.A. Grabowski, N. Leslie, R. Wenstrup, Enzyme therapy for Gaucher disease: the first 5 years, Blood Rev. 12 (1998) 115–133.

[5] C.A. Prows, N. Sanchez, C. Daugherty, G.A. Grabowski, Gaucher disease: enzyme therapy in the acute neuronopathic variant, Am. J. Med. Genet. 71 (1997) 16–21.

[6] R. Schiffmann, M.P. Heyes, J.M. Aerts, J.M. Dambrosia, M.C. Patterson, T. DeGraba, C.C. Parker, G.C. Zirzow, K. Oliver, G. Tedeschi, et al., Prospective study of neurological responses to treatment with macrophage-targeted glucocerebrosidase in patients with type 3 Gaucher's disease, Ann. Neurol. 42 (1997) 613–621.

[7] M. Aoki, Y. Takahashi, Y. Miwa, S. Iida, K. Sukegawa, T. Horai, T. Orii, N. Kondo, Improvement of neurological symptoms by enzyme replacement therapy for Gaucher disease type IIIb, Eur. J. Pediatr. 160 (2001) 63–64.

[8] T. Cox, R. Lachmann, C. Hollak, J. Aerts, S. van Weely, M. Hrebicek, F. Platt, T. Butters, R. Dwek, C. Moyses, et al., Novel oral treatment of Gaucher's disease with *N*-butyldeoxynojirimycin (OGT918) to decrease substrate biosynthesis, Lancet 355 (2000) 1481–1485.

[9] F.M. Platt, M. Jeyakumar, U. Andersson, D.A. Priestman, R.A. Dwek, T.D. Butters, Inhibition of substrate synthesis as a strategy for glycolipids lysosomal storage disease therapy, J. Inherit. Metab. Dis. 24 (2001) 275–290.

[10] J.Q. Fan, S. Ishii, N. Asano, Y. Suzuki, Accelerated transport and maturation of lysosomeal α-galactosidase A in Fabry lymphoblasts by an enzyme inhibitor, Nat. Med. 5 (1999) 112–115.

[11] L. Tominaga, Y. Ogawa, M. Taniguchi, K. Ohno, J. Matsuda, A. Oshima, Y. Suzuki, E. Nanba, Galactonojirimycin derivatives restore mutant human β-galactosidase activities expressed in fibroblasts from enzyme-deficient knockout mouse, Brain Develop. 23 (2000) 228–284.

[12] A.R. Sawkar, W.C. Cheng, E. Beutler, C.H. Wong, W.E. Balch, J.W. Kelly, Chemical chaperones increase the cellular activity of N370S β-glucosidase: a therapeutic strategy for Gaucher disease, Proc. Natl. Acad. Sci. U. S. A. 99 (2002) 15428–15433.

[13] S. Ogawa, M. Ashiura, C. Uchida, S. Watanabe, C. Yamazaki, K. Yamagishi, J. Inokuchi, Synthesis of potent β-D-glucocerebrosidase inhibitors: *N*-alkyl-β-valienamines, Bioorg. Med. Chem. Lett. 6 (1996) 929–932.

[14] J. Matsuda, O. Suzuki, A. Oshima, Y. Yamamoto, A. Noguchi, K. Takimoto, M. Itoh, Y. Matsuzaki, Y. Yasuda, S. Ogawa, Y. Sakata, E. Nanba, K. Higaki, Y. Ogawa, L. Tominaga, K. Ohno, H. Iwasaki, H. Watanabe, R.O. Brady, Y. Suzuki, Chemical chaperone therapy for brain pathology in G(M1)-gangliosidosis, Proc. Natl. Acad. Sci. U. S. A. (2003) 15912–15917.

[15] S. Ogawa, Y. Kobayashi, K. Kabayama, M. Jimbo, J. Inokuchi, Chemical modification of β-glucocerebrosidase inhibitor *N*-octyl-β-valienamine: synthesis and biological evaluation of *N*-alkanoyl and *N*-alkyl derivatives, Bioorg. Med. Chem. 6 (1998) 1955–1962.

[16] H. Lin, K. Ohno, Preclinical research of a new therapy for Gaucher's disease with F213I mutation, Zhonghua YiXue YiChuan Xue ZaZhi 20 (2003) 381–384.

[17] E.I. Ginns, F.P. Tegelaers, R. Barneveld, H. Galjaard, A.J. Reuser, R.O. Brady, J.M. Tager, J.A. Barranger, Determination of Gaucher's disease phenotypes with monoclonal antibody, Clin. Chim. Acta 131 (1983) 283–287.

[18] S. Ichisaka, K. Ohno, I. Yuasa, E. Nanba, H. Sakuraba, Y. Suzuki, Increased expression of β-hexosaminidase α chain in cultured skin fibroblasts from patients with carbohydrate-deficient glycoprotein syndrome type I, Brain Develop. 20 (1998) 302–306.

[19] Y. Eto, H. Ida, Clinical and molecular characteristics of Japanese Gaucher disease, Neurochem. Res. 24 (1999) 207–211.
[20] A.M. Vaccaro, M. Muscillo, M. Tatti, R. Salvioli, E. Gallozzi, K. Suzuki, Effect of a heat-stable factor in human placenta on glucosylceramidase, glucosylsphingosine glucosyl hydrolase, and acid β-glucosidase activities, Clin. Biochem. 20 (1987) 429–433.
[21] Y. Suzuki, A. Tsuji, K. Omura, G. Nakamura, S. Awa, M. Kroos, A.J. Reuser, Km mutant of acid α-glucosidase in a case of cardiomyopathy without signs of skeletal muscle involvement, Clin. Genet. 33 (1988) 376–385.
[22] Y. Sugimoto, H. Ninomiya, Y. Ohsaki, K. Higaki, J.P. Davies, Y.A. Ioannou, K. Ohno, Accumulation of cholera toxin and GM1 ganglioside in the early endosome of Niemann–Pick C1-deficient cells, Proc. Natl. Acad. Sci. U. S. A. 98 (2001) 12391–12396.
[23] L.S. Chin, M.C. Raynor, X. Wei, H.Q. Chen, L. Li, Hrs interacts with sorting nexin 1 and regulates degradation of epidermal growth factor receptor, J. Biol. Chem. 276 (2001) 7069–7078.
[24] A. Klein, M. Henseler, C. Klein, K. Suzuki, K. Harzer, K. Sandhoff, Sphingolipid activator protein D (sap-D) stimulates the lysosomal degradation of ceramide in vivo, Biochem. Biophys. Res. Commun. 200 (1994) 1440–1448.
[25] Y. Liu, Y.P. Wu, R. Wada, E.B. Neufeld, K.A. Mullin, A.C. Howard, P.G. Pentchev, M.T. Vanier, K. Suzuki, R.L. Proia, Alleviation of neuronal ganglioside storage does not improve the clinical course of the Niemann–Pick C disease mouse, Hum. Mol. Genet. 9 (2000) 1087–1092.
[26] M. Pasmanik-Chor, L. Madar-Shapiro, E.O. Stein, H. Aerts, S. Gatt, M. Horowitz, Expression of mutated glucocerebrosidase alleles in human cells, Hum. Mol. Genet. 6 (1997) 887–895.
[27] Y. Oda, N. Hosokawa, I. Wada, K. Nagata, EDEM as an acceptor of terminally misfolded glycoproteins released from calnexin, Science 299 (2003) 1394–1397.
[28] K.P. Zimmer, P. le Coutre, H.M. Aerts, K. Harzer, M. Fukuda, J.S. O'Brien, H.Y. Naim, Intracellular transport of acid β-glucosidase and lysosome-associated membrane proteins is affected in Gaucher's disease (G202R mutation), J. Pathol. 188 (1999) 407–414.

R00086058_BBADIS_62314

THE JOURNAL OF BIOLOGICAL CHEMISTRY
Vol. 279, No. 39, Issue of September 24, pp. 41114–41123, 2004
Printed in U.S.A.
© 2004 by The American Society for Biochemistry and Molecular Biology, Inc.

Skeletal Muscle FOXO1 (FKHR) Transgenic Mice Have Less Skeletal Muscle Mass, Down-regulated Type I (Slow Twitch/Red Muscle) Fiber Genes, and Impaired Glycemic Control*[S]

Received for publication, January 21, 2004, and in revised form, July 9, 2004
Published, JBC Papers in Press, July 21, 2004, DOI 10.1074/jbc.M400674200

Yasutomi Kamei‡§¶, Shinji Miura§, Miki Suzuki§, Yuko Kai§, Junko Mizukami‖, Tomoyasu Taniguchi‖, Keiji Mochida, Tomoko Hata‡‡, Junichiro Matsuda‡‡, Hiroyuki Aburatani§§, Ichizo Nishino¶¶, and Osamu Ezaki§**

*From the ‡PRESTO, Japan Science and Technology Agency, §Division of Clinical Nutrition, National Institute of Health and Nutrition, 1-23-1 Toyama, Shinjuku-ku, Tokyo 162-8636, ‖Lead Generation Research Laboratory, Tanabe Seiyaku Co., Ltd., 3-16-89 Kashima, Yodogawa-ku, Osaka 532-8505, **Bioresource Center, Institute of Physical and Chemical Research, 3-1-1 Koyadai, Tsukuba-shi, Ibaraki 305-0074, the ‡‡Department of Veterinary Science, National Institute of Infectious Diseases, 1-23-1 Toyama, Shinjuku-ku, Tokyo 162-8640, §§Research Center for Advanced Science and Technology, University of Tokyo, 4-6-1 Komaba, Meguro-ku, Tokyo 153-8904, and the ¶¶Department of Neuromuscular Research, National Institute of Neuroscience, National Center of Neurology and Psychiatry, 4-1-1 Ogawahigashi-cho, Kodaira, Tokyo 187-8502, Japan*

FOXO1, a member of the FOXO forkhead type transcription factors, is markedly up-regulated in skeletal muscle in energy-deprived states such as fasting and severe diabetes, but its functions in skeletal muscle have remained poorly understood. In this study, we created transgenic mice specifically overexpressing FOXO1 in skeletal muscle. These mice weighed less than the wild-type control mice, had a reduced skeletal muscle mass, and the muscle was paler in color. Microarray analysis revealed that the expression of many genes related to the structural proteins of type I muscles (slow twitch, red muscle) was decreased. Histological analyses showed a marked decrease in size of both type I and type II fibers and a significant decrease in the number of type I fibers in the skeletal muscle of FOXO1 mice. Enhanced gene expression of a lysosomal proteinase, cathepsin L, which is known to be up-regulated during skeletal muscle atrophy, suggested increased protein degradation in the skeletal muscle of FOXO1 mice. Running wheel activity (spontaneous locomotive activity) was significantly reduced in FOXO1 mice compared with control mice. Moreover, the FOXO1 mice showed impaired glycemic control after oral glucose and intraperitoneal insulin administration. These results suggest that FOXO1 negatively regulates skeletal muscle mass and type I fiber gene expression and leads to impaired skeletal muscle function. Activation of FOXO1 may be involved in the pathogenesis of sarcopenia, the age-related decline in muscle mass in humans, which leads to obesity and diabetes.

Skeletal muscle is the largest organ in the human body, comprising about 40% of the body weight. The mass and composition of skeletal muscle are critical for its functions, such as exercise, energy expenditure, and glucose metabolism (1, 2). Elderly humans are known to undergo a progressive loss of muscle fibers associated with diabetes, obesity, and decreased physical activity (sarcopenia) (3). In human skeletal muscle, there are two major classifications of fiber type: type I (slow-twitch oxidative, so-called red muscle) and type II (fast-twitch glycolytic, so-called white muscle) fibers (2). Mass, fiber size, and fiber composition in adult skeletal muscle are regulated in response to changes in physical activity, environment, or pathological conditions. For example, space flight experiments using rats showed a reduction in total skeletal muscle mass of up to 37% as well as a significant loss of contractile proteins in type I but not type II fibers by 1–2 weeks of microgravity (4). Furthermore, the ratio of type I to type II fibers is associated with obesity and diabetes; the number of type I fibers is reduced in obese subjects and diabetic subjects compared with that in controls (5–7).

Skeletal muscle mass is positively regulated by hormones such as insulin-like growth factors (IGFs)[1] and growth hormone (8). Induction of hypertrophy in adult skeletal muscle by increased load is accompanied by the increased expression of IGF-1 (9). Systemic administration of IGF-1 results in increased skeletal muscle protein and reduced protein degradation (10). In addition, overexpression of IGF-1 blocks the age-related loss of skeletal muscle (11). Supplementation of IGF-1 to muscle cells *in vitro* promotes myotube hypertrophy, suggesting that hypertrophy can be mediated by autocrine- or paracrine-produced IGF-1 (12). Thus, delivery of the *IGF-1* gene specifically into skeletal muscle has been proposed as a genetic therapy for skeletal muscle disorders. A better understanding of the role of IGF-1 in skeletal muscle is therefore of great importance.

Specialized/differentiated myofiber phenotypes, including type I and type II fibers, are plastic and are physiologically

* This work was supported in part by research grants from the Japanese Ministry of Health, Labor, and Welfare (Tokyo) and by a grant from the Promotion of Fundamental Studies in Health Sciences of the Organization for Pharmaceutical Safety and Research. The costs of publication of this article were defrayed in part by the payment of page charges. This article must therefore be hereby marked "*advertisement*" in accordance with 18 U.S.C. Section 1734 solely to indicate this fact.

[S] The on-line version of this article (available at http://www.jbc.org) contains Information 1 and 2.

¶ To whom correspondence should be addressed: Division of Clinical Nutrition, National Institute of Health and Nutrition, 1-23-1 Toyama, Shinjuku-ku, Tokyo 162-8636, Japan. Tel.: 81-3-3203-5725; Fax: 81-3-3207-3520; E-mail: ykamei@nih.go.jp.

[1] The abbreviations used are: IGF, insulin-like growth factor; CaMK, calmodulin-dependent kinase; PGC-1α, peroxisome proliferator activated receptor-γ coactivator-1α; STZ, streptozotocin; MLC, myosin light chain; mtCK, mitochondrial creatine kinase; IGFBP, IGF-binding protein; COX, cytochrome *c* oxidase; DEXA, dual energy X-ray absorptiometry; EDL, extensor digitorum longus.

This paper is available on line at http://www.jbc.org

controlled by variations in motor neuron activity. The influence of motor neuron activity on different types of skeletal muscle fibers is considered to be transduced via calcium signaling and downstream molecules such as calcineurin and the calmodulin-dependent kinase (CaMK) pathway (13). Signals generated by calcium/calcineurin/CaMK augment the transactivating function of Mef2 and/or NFAT and enhance type I fiber-specific gene expression (13–18). More recently, it has been shown that a nuclear receptor cofactor (19, 20), peroxisome proliferator activated receptor-γ coactivator-1α (PGC-1α) (21), drives the formation of type I fibers. Specifically, in transgenic mice expressing PGC-1α, type II fibers are red in color, and PGC-1α activates expression of type I fiber-specific genes (22). We also reproduced the PGC-1α-induced red appearance of skeletal muscle; both type I and type II fibers appear redder in transgenic mice overexpressing PGC-1α in skeletal muscle (23).

FOXO1 (FKHR), FOXO4 (AFX), and FOXO3a (FKHRL1) are a subfamily of the forkhead type transcription factors (24, 25). FOXO1 was originally cloned from a rhabdomyosarcoma because of its aberrant fusion with another transcription factor, PAX3, resulting from a chromosomal translocation (26). Recent studies have shown that the FOXO protein can also act as a cofactor of nuclear receptor activity (27–30). FOXO family members have been shown to regulate various cellular functions. FOXOs influence the transcription of genes involved in metabolism (31–34), the cell cycle (35, 36), and apoptosis (37, 38). In addition, FOXO1 can modulate cell differentiation; the constitutive active form of FOXO1 prevents the differentiation of preadipocytes (39) and stimulates myotube fusion of primary mouse myoblasts (40). Moreover, a FOXO1 knockout mouse has been reported; *Foxo1* haploinsufficiency restores insulin sensitivity and rescues the diabetic phenotype in insulin-resistant mice by reducing the hepatic expression of glucogenetic genes and by increasing the adipocytic expression of insulin-sensitizing genes (41). We have shown that FOXO1 expression is increased in skeletal muscle in energy-deprived states, such as in fasting mice, in mice with streptozotocin (STZ)-induced diabetes, and in mice after treadmill running (42). However, the physiological role of FOXO1 in skeletal muscle is still unclear. Although many studies have been performed using cultured cells, studies using animals with genetic modifications focused to the skeletal muscle remain to be conducted in order to understand the function of the FOXO family proteins *in vivo*. Meanwhile, it has been reported that FOXO1 and PGC-1α can physically interact and regulate gene expression in the liver (43). Given that PGC-1α is important for the differentiation of type I fibers, FOXO1 might be involved in this process. (Hereafter, we use "differentiation of muscle fiber" to mean "a switch from one fiber type to another fiber type.") On the other hand, a genetic study of *Caenorhabditis elegans* showed that DAF16, the worm counterpart of FOXO, functions as a suppressor of insulin receptor-like signaling (44). Thus, the FOXO family may act negatively in mammals as a downstream player in insulin or IGF signaling. As IGF-1 plays an important role in controlling skeletal muscle mass, FOXO1 might also be involved in this process.

To gain insight into the potential role of FOXO1 in skeletal muscle, including the control of skeletal muscle mass and the control of differentiation of muscle fiber type, we established transgenic mice specifically overexpressing FOXO1 in their skeletal muscle. Most interestingly, these mice showed reduced skeletal muscle mass, and the muscle was paler in color. Histochemical, physiological, and microarray analyses of these FOXO1 transgenic mice showed that FOXO1 is involved in the regulation of skeletal muscle mass and type I fiber gene expression. In addition, our results suggest that FOXO1 activation may play a role in the impairment of skeletal muscle function including glycemic control.

EXPERIMENTAL PROCEDURES

RNA Analysis—Northern blot analyses were performed as described previously (42). The cDNA probes for Gadd45α (GenBank™ accession number, U00937), troponin C (slow) (M29793), troponin T (slow) (AV213431), myosin light chain (MLC) (slow) (M91602), myoglobin (X04405), mitochondrial creatine kinase (mtCK, AV250974), F_0F_1-ATPase (AF030559), MLC (fast) (U77943), troponin I (fast) (J04992), troponin T (fast) (L48989), cathepsin L (X06086), IGF-binding protein 5 (IGFBP5) (L12447), MuRF1 (AF294790), and atrogin 1 (AF441120) were obtained by reverse transcription-PCR. The PCR primers used are as follows: Gadd45α, forward, 5′-TCGCACTTGCAATATGACTT-3′, and reverse, 5′-CGGATGCCATCACCGTTCCG-3′; troponin C (slow), forward, 5′-AGCTGCGGTAGAACAGTTGA-3′, and reverse, 5′-TCACCTGTGGCCTGCAGCAT-3′; troponin T (slow), forward, 5′-TTCTGTCCAACATGGGAGCT-3′, and reverse, 5′-TCGGAATTTCTGGGCGTGGC-3′; MLC (slow), forward, 5′-GAGTTCAAGGAAGCCTTCAC-3′, and reverse, 5′-CTGCGAACATCTGGTCGATC-3′; myoglobin, forward, 5′-CACCATGGGGCTCAGTGATG-3′, and reverse, 5′-CTCAGCCCTGGAAGCCTAGC-3′; mtCK, forward, 5′-AAAGGAAGTGGAACGATTAA-3′, and reverse, 5′-TTGATGTCTTGGCCTCTCTC-3′, F_0F_1-ATPase, forward, 5′-ACTGACCCTGCCCCTGCAAC-3′, and reverse, 5′-CAAGGCTCTTGTGTGGCCTG-3′, MLC (fast), forward, 5′-AGGGATGGCATTATCGACAA-3′, and reverse, 5′-CAGATGTTCTTGTAGTCCAC-3′; troponin I, (fast), forward, 5′-AGGAAAGCCGCCGAGAATCT-3′, and reverse, 5′-TACTGGGGAAGTGGGCAGTT-3′; troponin T (fast), forward, 5′-CAGCAAAGAATTCGCGCTGA-3′, and reverse, 5′-GGCCTTCTTGCTGTGCTTCT-3′; cathepsin L, forward, 5′-CGGAGGAGTCTTACCCCTAT-3′, and reverse, 5′-CTACCCATCAATTCACGACA-3′; IGFBP5, forward, 5′-GCCTATGCCGTACCGGCTCA-3′, and reverse, 5′-CTTCACAGCCTCAGCCTTCA-3′; MuRF1, forward, 5′-ATGAACTTCACGGTGGGTTT-3′, and reverse, 5′-TCAGTGCAGGCCTGAGCCTT-3′; and atrogin 1, forward, 5′-ATGCCGTTCCTTGGGCAGGA-3′, and reverse, 5′-TCAGAACTTGAACAAATTGA-3′. FOXO1, FOXO3a, and FOXO4 cDNA probes were prepared as reported previously (42). COXII, COXIV, Mef2c, PGC-1α, and glucose transporter 4 cDNA probes were prepared as described previously (23). NFAT (IMAGE clone 4109469) and CaMK IIβ (IMAGE clone 5014712) cDNA probes were purchased from Invitrogen.

Generating Transgenic Mice—The human skeletal muscle α-actin promoter (45) was provided by Drs. E. D. Hardeman and K. Guven (Children's Medical Research Institute, Australia). The human FOXO1 cDNA was as described previously (42). The transgene (Fig. 1A) was excised from agarose gel and purified for injection (2 ng μl^{-1}). Fertilized eggs were recovered from C57BL/6 females crossed with C57BL/6 males and microinjected at Japan SLC Inc. (Hamamatsu, Japan). The mice were maintained at a constant temperature of 22 °C with fixed artificial light (12-h light and 12-h dark cycle). Care of the mice was conducted in accordance with the institutional guidelines.

Body Composition Analysis—Mice were anesthetized with pentobarbital sodium, Nembutal (0.08 mg/g body weight, Abbott), and scanned with a Lunar PIXI mus2 densitometer (Lunar Corp., Madison, WI), equipped for dual energy x-ray absorptiometry (DEXA) (46).

Immunoblotting—Protein extracts from skeletal muscle were prepared by centrifugation of the tissue homogenates as described previously (47). Protein extracts (30 μg) separated by SDS-PAGE were electrophoretically transferred to Immobilon P membranes (Millipore, Bedford, MA). Immunoblotting was performed by using goat anti-FOXO1 IgG (N-18, Santa Cruz Biotechnology, Inc. Santa Cruz, CA), goat anti-troponin I (slow) (C-19, Santa Cruz Biotechnology), goat anti-troponin I (fast) (C-19, Santa Cruz Biotechnology), goat anti-myoglobin (M-109, Santa Cruz Biotechnology), or rabbit anti-PGC-1α (C terminus, Calbiochem) as primary antibodies (1:1000) and anti-goat IgG or anti-rabbit IgG conjugated with horseradish peroxidase as secondary antibodies (1:1000). Bands were visualized with the enhanced chemiluminescence system (Amersham Biosciences).

Histological Analyses—Skeletal muscle (soleus) samples were frozen in liquid nitrogen-cooled isopentane, and transverse serial sections were stained with ATPase at pH 4.3 to detect type I fibers and at pH 10.5 to detect type II fibers (48). The ratio of type I fibers to type II fibers and the size (area) of skeletal muscle cells were determined by counting cell numbers in six randomly selected cross-section areas (each 900 μm^2) stained with ATPase at pH 4.3.

Blood Analysis—Blood samples were obtained from mice tail tips for hormone and metabolite determination under feeding conditions. Immunoreactive insulin was measured by an insulin assay kit (Morinaga,

Kanagawa, Japan), free fatty acid by NEFA C-test Wako (Wako Biochemicals, Osaka, Japan), lactate by the lactate reagent (Sigma), and glucose by the TIDEX glucose analyzer (Sankyo, Tokyo, Japan).

Running Wheel Activity—Mice were housed individually in cages (9 × 22 × 9 cm) equipped with a running wheel (20-cm in diameter, Shinano Co., Tokyo, Japan). Each wheel revolution was registered by a magnetic switch, which was connected to a counter. The number of revolutions was recorded daily for 6 days.

Oral Glucose and Insulin Tolerance Test—For the oral glucose tolerance test, D-glucose (1 mg/g of body weight, 10% (w/v) glucose solution) was administered with a stomach tube after an overnight fast. Blood samples were obtained by cutting the tail tip before and 30, 60, and 120 min after glucose administration. For the insulin tolerance test, human insulin (Humulin R; Lilly) was injected intraperitoneally (0.75 milliunits/g of body weight) into fed animals. Blood glucose concentrations were measured using a TIDEX glucose analyzer (Sankyo, Tokyo, Japan).

Microarray Analyses—RNA was isolated from skeletal muscle (quadriceps) of sex- and age-matched FOXO1 mice (A1 and A2 lines) and control mice (males at 4 months of age, RNA from three mice of each group were combined). Each of the combined samples was hybridized to the Affymetrix MGU74A microarray, which contains 12,489 genes including ESTs, and analyzed with the Affymetrix Gene Chip 3.1 software as described previously (49). Of the 12,489 genes including ESTs analyzed, 2500 (nontransgenic control mice), 2490 (line A1, transgenic), and 2510 (line A2, transgenic) genes were expressed at a substantial level (absolute call is present and average difference is above 150). Genes were classified on the basis of the biological function of the encoded protein, using a previously established classification scheme (50). The classification scheme was composed of seven major functional categories and several minor functional categories within the major categories.

Statistical Analyses—Statistical comparisons of data from the experimental groups were performed by the one-way analysis of variance, and groups were compared using the Fisher's protected least significant difference test (Statview 5.0, Abacus Concepts, Inc., Berkeley, CA). The glucose and insulin tolerance curves were compared by repeated measure analysis (Statview 5.0, Abacus Concepts). When significant, groups were compared by the Fisher's protected least significant difference test. Statistical significance was defined as $p < 0.05$.

RESULTS

Creation of FOXO1 Mice—The human skeletal muscle α-actin promoter (45) was used to drive the expression of the human *FOXO1* transgene in mice (Fig. 1*A*). During development, cardiac muscle α-actin is the predominant isoform of sarcomeric α-actin in mice, and the switch to skeletal muscle α-actin occurs postpartum (45). Thus, by using the skeletal muscle α-actin promoter, the possibility that embryonic expression of FOXO1 might interfere with development was minimized. We obtained two independent lines of transgenic mice (lines A1 and A2). Southern blot analysis of DNA obtained from mouse tails was performed as shown in Fig. 1*B*. The transgene copy number of each animal was estimated by densitometric scanning of the autoradiographs from the Southern blots.

Expression of the *FOXO1* transgene was evaluated by Northern blot analysis with RNA isolated from the tissues of FOXO1 mice and age-matched control mice at 8 weeks of age (Fig. 1*C*). The use of this promoter resulted in predominantly high expression levels of the *FOXO1* transgene in skeletal muscle (about 3.5 kb). The A2 line showed expression levels of the *FOXO1* transgene in skeletal muscle that were similar to or slightly higher than that in the A1 line. Transgene expression was observed not only in the gastrocnemius and quadriceps but also in other areas of skeletal muscle including the tibialis anterior, extensor digitorum longus (EDL), and soleus (not shown). The blot was then re-hybridized with a cDNA probe of Gadd45α, an authentic target gene of FOXO1 (51, 52). As expected, induction of the expression of Gadd45α was observed in skeletal muscle but not in other tissues in both FOXO1 transgenic mouse lines (Fig. 1*C*), indicating that the transgene expressed a functional FOXO1 protein. By using an antibody that recognizes both human and mouse FOXO1, we confirmed

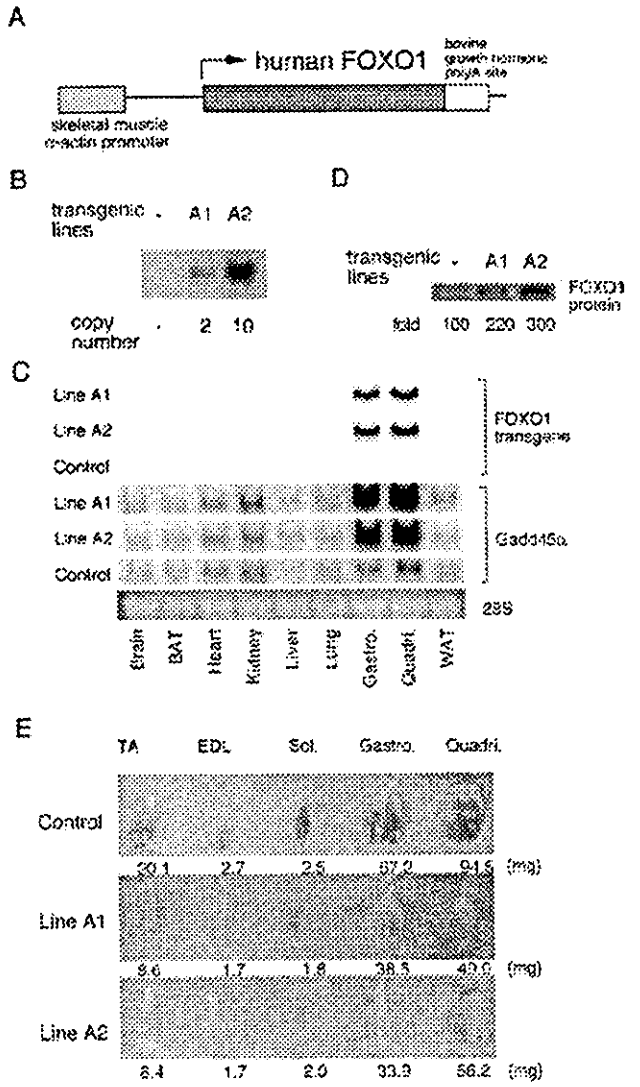

FIG. 1. **Creation of FOXO1 transgenic mice.** *A*, map of the 5-kb construct used for transgenic microinjection. The transgene was under the control of the human skeletal muscle α-actin promoter and included exon 1 and the intron of the human skeletal muscle α-actin gene as well as the bovine growth hormone polyadenylation site (45). *B*, characterization of FOXO1 mice. Two transgenic lines, *A1* and *A2*, were identified by Southern blot analyses of DNA obtained from the tail of each mouse. The copy number was 2 for *A1* and 10 for *A2*, as estimated by densitometric scanning of the autoradiographs of the Southern blot. *C*, expression of the *FOXO1* transgene in mice. Northern blot analysis of human FOXO1 mRNA expression in tissues from FOXO1 mice (*line A1* and *A2*) and nontransgenic control mice. RNAs from brain, brown adipose tissue (*BAT*), heart, kidney, liver, lung, skeletal muscle (gastrocnemius (*Gastro.*) and quadriceps (*Quadri.*)), and white adipose tissue (*WAT*) were analyzed. The blots were re-hybridized with the *Gadd45α* probe. Each lane contained 20 μg of total RNA. *28 S* ribosomal RNA staining of a sample from control mice is shown. Similar staining was observed in samples from transgenic mice (not shown). *D*, expression of the FOXO1 protein in the skeletal muscle of FOXO1 mice. Protein extracts (30 μg per lane) were subjected to SDS-PAGE. The FOXO1 protein was detected by immunoblotting. The densitometric ratio is shown below the autoradiogram (the control was set as *100*). *E*, comparison of representative samples of dissected skeletal muscle (*TA*, tibialis anterior; *Sol*, soleus; *Gastro*, gastrocnemius; *Quadri*, quadriceps) between FOXO1 mice and littermate control mice. Legs were removed from 4-month-old (*lines A1* and *A2*) transgenic mice and age-matched control mice. Tibialis anterior, gastrocnemius, and quadriceps contain a mixture of type I and II fibers; EDL is enriched in type II fibers, and soleus is enriched in type I fibers (control). Average dry mass ($n = 3$ in each group) is shown below the panel. Muscles were smaller in size and paler in color in FOXO1 mice than in control mice.